Pump–probe spectrum of molecular assemblies of arbitrary structure and dimension

Juzeliūnas, Gediminas; Knoester, Jasper

Published in:
Journal of Chemical Physics

DOI:
10.1063/1.480798

Pump–probe spectrum of molecular assemblies of arbitrary structure and dimension

Gediminas Juzeliūnas
Institute of Theoretical Physics and Astronomy, A. Goštauto 12, Vilnius 2600, Lithuania

Jasper Knoester
Institute for Theoretical Physics and Materials Science Center, University of Groningen, Nijenborgh 4, 9747 AG Groningen, The Netherlands

(Received 12 August 1999; accepted 28 October 1999)

Using the hard-core boson approach, we study the pump-probe spectrum of molecular assemblies carrying Frenkel excitons of arbitrary structure and dimension. We present a rigorous justification of the hard-core boson approach by using the Agranovich–Toshich transformation from paulions to bosons. The resulting two-exciton Green function is used to derive a general expression of the assembly's pump–probe spectrum. We show that this expression considerably simplifies for ordered systems occupying a lattice, where we allow for the occurrence of more than one equivalent molecule in the unit cell (Davydov components). Explicit semianalytical expressions are given for the pump–probe spectrum of linear chains with alternating dipoles, ring aggregates, chains with a herringbone structure, and monolayers. In the analysis of these expressions, we focus on the overall shape of the spectrum and on the effects of probe polarization. It is shown that relaxation during the pump–probe delay time may drastically affect the pump–probe spectrum. © *2000 American Institute of Physics.* [S0021-9606(00)70804-X]

I. INTRODUCTION

The collective optical dynamics of molecular assemblies supporting Frenkel excitons[1–3] is a field that continues to attract attention. Among the systems arousing most interest are *J* aggregates of cyanine dyes, Langmuir–Blodgett monolayers, and biomolecular systems such as antenna complexes consisting of chlorophyll molecules. Recently, many theoretical[4–15] and experimental[16–24] studies have been devoted to the pump–probe spectrum of these systems. In the weak-pump limit, this is a third-order nonlinear optical technique, which allows one to probe transitions between one-exciton states and two-exciton states. For *J* aggregates, this transition is blueshifted compared to the ground state absorption band (the *J* band), which is a consequence of the fact that excitons are paulions, i.e., two excitations cannot reside on the same molecule. For one-dimensional *J* aggregates, this blueshift allows one to estimate the extent of the exciton wave function imposed by the size of the aggregate or by static disorder, provided that dynamic (homogeneous) broadening does not dominate the spectrum.[4,12–14,22]

Most of the work on molecular aggregates has been performed in the context of one-dimensional Frenkel exciton models, which has often led to a good comparison between theory and experiment. Still, the dimensionality of *J* aggregates is not a settled issue. Although absorption experiments in streaming solutions[25] and on mixed PIC-aza-PIC aggregates[26] support a one-dimensional structure, experiments involving relaxation, such as exciton–exciton annihilation[27–29] and temperature dependent fluorescence,[30] question this picture. It is conceivable that on the length scale of exciton coherence, which is relevant to coherent optical experiments, *J* aggregates behave as one-dimensional, whereas on larger length scales, probed by diffusion, they reveal a more complicated structure. Such a hierarchy of length scales, involving domains and meso-aggregates has been suggested by several authors.[27,29,31–33] In addition, techniques exist which produce well-defined assemblies with a structure that is not linear. As examples, we mention Langmuir–Blodgett films,[34] which obviously call for a two-dimensional description, and the helical aggregates lying on a cylindrical surface reported in Refs. 35 and 36.

In this paper, motivated by the above observations, we will study the pump–probe spectrum for Frenkel exciton systems of arbitrary dimension and structure. Although our general formulation also applies in the presence of disorder, we will pay special attention, to the case of ordered aggregates, where we derive explicit (semi-)analytical expressions for the pump–probe spectrum of various types of assembly structures. We believe that their simplicity renders these expressions useful tools in the analysis of experiments on more complicated molecular structures.

Our method is based on the hard-core boson approach, in which the paulions are treated as bosons, with an infinite on-site repulsion taking care of the kinematic interaction (the exclusion principle) felt by the paulions. This method was first proposed by Van Kranendonk[37] when dealing with spin waves, but was criticized as naive by Dyson.[38] Subsequently, working in the context of Frenkel excitons, Agranovich and Toshich[2,39] suggested an exact (yet complicated) transformation converting paulions to bosons, which lended further support to the hard-core boson approach. The method has also been advocated by Mukamel and co-workers. Leegwater and Mukamel introduced the hard-core potential to calculate the general four-wave mixing optical susceptibility of molecular

assemblies,[40] while more recently the pump–probe spectrum was also studied using this approach.[13]

In spite of the amount of earlier work, in our opinion a rigorous justification of the hard-core boson approach is still lacking. In this paper, we fill this void by using the Agranovich–Toshich transformation and by showing that the many-boson interactions which result from this transformation may, up to the two-particle level, indeed be replaced by a hard-core interaction. Crucial ingredients in this derivation are the Heitler–London approximation and the fact that third-order optical response only is sensitive to one- and two-exciton states.

The second goal of this paper is to use the hard-core boson method to derive explicit semianalytical expressions for the pump–probe spectrum of various examples of ordered aggregate structures. In this analysis we account for structures with more than one molecule in a unit cell. This situation often occurs in organic molecular systems and leads to the well-known formation of Davydov components in the one-exciton subspace.[1] The effect on two-exciton states and the pump–probe spectrum has thus far not been considered.

The outline of this paper is as follows. In Sec. II, we present the Hamiltonian, justify the hard-core boson approach, and calculate the two-exciton Green function using this method. This Green function is used in Sec. III to derive the formal expression for the differential absorption spectrum. In Sec. IV, we restrict ourselves to ordered aggregates and derive an expression for the pump–probe spectrum which only involves the manipulation (diagonalization and inversion) of $S\times S$ matrices, where S is the number of molecules per unit cell. Sections V–VII are devoted to the explicit expressions and their analysis for the pump–probe spectra of specific examples. We consider linear chains with alternating dipoles (Sec. V A), ring aggregates (Sec. V B), linear aggregates with a herringbone structure (two molecules per unit cell, Sec. VI), and molecular monolayers (Sec. VII). One of the aspects receiving particular attention is the dependence on the probe polarization. Finally, we conclude in Sec. VIII. Appendixes A, B, and C contain technical details that are of importance but which would break the line of the main text too much if included there.

II. GENERAL FORMULATION

A. Hamiltonian and bosonification

We consider an aggregate of $\mathcal{N}$ two-level molecules with electronic excitations described by the Frenkel exciton Hamiltonian:[1–3]

$$H_{\rm exc}=\sum_n \varepsilon_n P_n^\dagger P_n+\sum_{n\neq n'} L_{n,n'}P_n^\dagger P_{n'}. \tag{1}$$

Here, $P_n^\dagger$ (P_n) is the Pauli operator for creation (annihilation) of an electronic excitation, with energy ε_n, at the molecule n, while $L_{n,n'}$ is the excitation transfer interaction between the molecules n and n'. At this stage, we do not impose any restriction on the system's dimension and structure; in addition, no translational symmetry is assumed.

In the above Hamiltonian, we have invoked the Heitler–London approximation, which neglects terms of the form $L_{n,n'}P_n^\dagger P_{n'}^\dagger$ and $L_{n,n'}P_nP_{n'}$.[1–3,41] The effect of such terms is small in exciton systems, owing to the fact that the molecular transition frequencies are typically much larger (by one to two orders of magnitude) than the transfer interactions. Within this approximation, the eigenstates of the Hamiltonian can be classified according to the number of excitations shared by the molecules. In particular, the ground state $|g\rangle$ is the state with all molecules in their ground state. The lowest excitations occur in a band of one-exciton states, in which the molecules share one excitation. The next higher band is the two-exciton band, etc. This classification will be a crucial element in the justification of the hard-core boson approach.

As is well-known, the Pauli operators $P_n^\dagger$ and P_n obey mixed Fermi and Bose commutation relations.[1–3] In particular, they behave as bosons if they belong to different sites, whereas for operators belonging to the same site, Fermi commutation relations apply. The latter describes the exclusion of doubly excited molecules (Pauli exclusion). By using the Agranovich–Toshich transformation, however, it is possible to represent the Pauli operators in terms of Bose operators $a_n^\dagger$ and a_n:[2,39,42,43]

$$P_n^\dagger=a_n^\dagger\left[\sum_{\nu=0}^{\infty}\frac{(-2)^\nu}{(1+\nu)!}(a_n^\dagger)^\nu(a_n)^\nu\right]^{1/2}, \tag{2}$$

and the hermitian conjugate for P_n. Although this transformation is exact, the expansion contains many-boson operators (quartic and higher order), which complicates its practical use. As we will restrict ourselves to nonlinear optical spectroscopies of order three or lower, however, it suffices to give an exact description of states that are one- and two-photon allowed from the ground state. These are the one- and two-exciton states. Thus, it is sufficient to retain the $\nu=0$ and $\nu=1$ terms in Eq. (2), leading to the Holstein–Primakov transformation:

$$P_n^\dagger=a_n^\dagger(1-a_n^\dagger a_n)^{1/2}=a_n^\dagger(1-a_n^\dagger a_n), \tag{3}$$

where the last equality holds because we limit ourselves to one- and two-particle states, so that $P_n^\dagger$ operates at most on a one-particle state.

The Hamiltonian Eq. (1) may now be rewritten in terms of Bose operators as

$$H_{\rm exc}=H_0+V_{\rm kin}, \tag{4}$$

with

$$H_0=\sum_n \varepsilon_n a_n^\dagger a_n+\sum_{n\neq n'} L_{n,n'}a_n^\dagger a_{n'} \tag{5}$$

and

$$V_{\rm kin}=-\sum_n \varepsilon_n a_n^\dagger a_n^\dagger a_n a_n-\sum_{n\neq n'} L_{n,n'}(a_n^\dagger a_n^\dagger a_n a_{n'}+a_n^\dagger a_{n'}^\dagger a_{n'}a_{n'}). \tag{6}$$

H_0 describes a system of noninteracting Bose excitons, whereas the operator $V_{\rm kin}$ introduces the kinematic interaction between these bosons. The role of the latter interaction is to cancel exactly any contributions of states of the form

$a_n^\dagger a_n^\dagger|g\rangle$, in which two bosons occur at one molecule. Such states are unphysical in the sense that they do not have an equivalent in the original (physical) paulion system; they rather arise as auxiliary states after the transformation to bosons. Due to the kinematic interaction, unphysical states are not coupled to the physical ones: $H_{\rm exc}a_n^\dagger a_n^\dagger|g\rangle=0$.

B. Green operator and the hard-core boson method

In order to calculate the pump–probe spectrum, we will need the Green operator in the one- and two-exciton subspace. The general Green operator is given by

$$G_{\rm exc}(x)=(x-H_{\rm exc}+i\eta)^{-1} \tag{7}$$

with $\eta\rightarrow+0$. In the two-exciton subspace, the kinematic interaction $V_{\rm kin}$ renders the calculation of $G_{\rm exc}$ nontrivial. This problem may be solved in two steps. First, we replace the kinematic interaction in Eq. (4) for $H_{\rm exc}$ by a hard-core potential between the bosons. This leads to the new ''hard-core boson'' Hamiltonian

$$H_{\rm hcb}=H_0+AQ, \tag{8}$$

with $A\rightarrow\pm\infty$ and

$$Q=\frac{1}{2}\sum_n a_n^\dagger a_n^\dagger a_n a_n, \tag{9}$$

the operator for projection onto the unphysical states. It appears to be intuitive that the hard-core potential added to the noninteracting boson term H_0 takes care of the Pauli exclusion principle for two excitons residing at the same site. In Appendix A, we prove rigorously that this is indeed the case. In particular, we show that the Green operator $G_{\rm exc}$ for the original Hamiltonian *within the subspace of one and two excitons* equals the Green operator for the hard-core boson model:

$$G_{\rm exc}(x)=G_{\rm hcb}(x)\equiv(x-H_{\rm hcb}+i\eta)^{-1}. \tag{10}$$

It should be realized that this identification of the original paulion system with the hard-core boson system depends crucially on the fact that we could classify the eigenstates of the original Hamiltonian according to the number of particles (paulions) shared by the molecules and that we only need the one- and two-particle states to calculate the pump–probe spectrum at relatively weak pump pulses. For spin systems, the Heitler–London approximation is not valid (the site energy vanishes in zero magnetic field) and the steps between Eqs. (2) and (6) are meaningless.

The second step in solving the two-exciton Green function lies in expressing $G_{\rm hcb}$ in terms of the Green operator G_0 for the free Bose excitons by using the Dyson equation. In Appendix B, we show how this can be done quite generally and in a somewhat more formal way than was used in Ref. 40. The result reads

$$G_{\rm hcb}=G_0-G_0(QG_0Q)^{-1}G_0, \tag{11}$$

with

$$G_0=(x-H_0+i\eta)^{-1}. \tag{12}$$

In Eq. (11), the operator $(QG_0Q)^{-1}$ is to be understood as the inverse of the Green operator G_0 projected on the subspace of unphysical states, i.e., $(QG_0Q)(QG_0Q)^{-1}=Q$. The action of the operator $(QG_0Q)^{-1}$ on the subspace of physical states is understood to yield zero. Combining Eqs. (10) and (11), we now have obtained the Green operator within the one- and two-exciton subspace.

III. GENERAL EXPRESSION FOR THE PUMP–PROBE SPECTRUM

In this section, we will derive a general expression for the weak-pulse pump–probe spectrum, which is valid for arbitrary dimension and structure of the aggregate as well as for arbitrary realization of static disorder. The pump–probe or differential absorption spectrum is defined as

$$\Delta I^{\rm in}(E)=I^{\rm in}(E)-I^g(E). \tag{13}$$

Here, $I^{\rm in}(E)$ denotes the linear probe absorption at photon energy E of the system which has been brought into the state $|{\rm in}\rangle$ by the pump pulse, while $I^g(E)$ is the ground state linear absorption spectrum (i.e., the probe absorption spectrum taken in the absence of a pump). In the weak-pulse case, $|{\rm in}\rangle$ is a one-exciton state. The above approach treats the third-order nonlinear spectrum as a sequence of two linear absorption processes, which implies the neglect of coherent artifacts.[44]

If the spectra are taken by resolving the absorption of a spectrally broad (white) probe pulse, they take the form

$$I^{\rm in}(E)=\sum_{\rm fin}\pm|\langle{\rm fin}|M|{\rm in}\rangle|^2\delta(E_{\rm in}-E_{\rm fin}\pm E). \tag{14}$$

Here, M denotes the total dipole operator of the aggregate which, for aggregates small compared to an optical wavelength, is given by

$$M=\sum_n \mu_n(P_n^\dagger+P_n), \tag{15}$$

with μ_n the (real) transition dipole matrix element, along the direction of the polarization of the light, of molecule n. Furthermore, the sum in Eq. (14) extends over all final states, $|{\rm fin}\rangle$, which are dipole allowed from the initial state $|{\rm in}\rangle$. Both $|{\rm in}\rangle$ and $|{\rm fin}\rangle$ are eigenstates of the Hamiltonian $H_{\rm exc}$, with energies $E_{\rm in}$ and $E_{\rm fin}$, respectively. If $E_{\rm in}<E_{\rm fin}$, the $+$ sign is selected in the δ function in Eq. (14) and, correspondingly, the upper $(+)$ sign is selected for the prefactor occurring under the summation over final states: the process then corresponds to real (positive) absorption. In the opposite case, we are dealing with stimulated emission, giving a negative contribution to the absorption spectrum. $I^g(E)$ is simply a special case of Eq. (14) with $|{\rm in}\rangle$ replaced by $|g\rangle$. Then, of course, stimulated emission cannot occur. Thus, the weak-pulse pump–probe spectrum shows positive resonances at energies of allowed transitions between the one-exciton $|{\rm in}\rangle$ and the two-exciton band (induced absorption) and negative resonances at all one-exciton energies (bleaching of the ground state and stimulated emission).

Using the delta function representation: $\delta(x)=-\pi^{-1}\,{\rm Im}(x+i\eta)^{-1}$ with $\eta\rightarrow+0$, we may rewrite Eq. (14) as

$$I^{\mathrm{in}}(E)=\pi^{-1}\,\mathrm{Im}\sum_{\mathrm{fin}}\ \mp\langle \mathrm{in}|M|\mathrm{fin}\rangle \times(E_{\mathrm{in}}\pm E-E_{\mathrm{fin}}+i\eta)^{-1}\langle \mathrm{fin}|M|\mathrm{in}\rangle =-\pi^{-1}\,\mathrm{Im}\langle \mathrm{in}|MG_{\mathrm{exc}}(y_+)M|\mathrm{in}\rangle +\pi^{-1}\,\mathrm{Im}\langle \mathrm{in}|MG_{\mathrm{exc}}(y_|)M|\mathrm{in}\rangle, \tag{16}$$

with

$$y_\pm=E_{\mathrm{in}}\pm E. \tag{17}$$

Equation (16) defines the absorption spectrum from an arbitrary initial state in terms the Green operator Eq. (7) and the dipole operator Eq. (15) formulated for the paulions. The next step is to rewrite Eq. (16) in terms of operators appropriate to the hard-core boson system. To this end, we take advantage of Eq. (10) demonstrating the equivalence of the original and the hard-core Green operators ($G_{\mathrm{exc}}=G_{\mathrm{hcb}}$) in the subspace of one- and two-particle states (which are the only relevant states in the weak-pulse experiment). Furthermore, within this subspace, Eq. (3) may be used to write the dipole operator as

$$M=\sum_n\ \mu_n[a_n^\dagger(1-a_n^\dagger a_n)+(1-a_n^\dagger a_n)a_n]. \tag{18}$$

Finally, introducing $R=I-Q$, the operator for projection on the space of physical states, and

$$M_+=M_-^\dagger\equiv\sum_n\ \mu_n a_n^\dagger, \tag{19}$$

it is easily shown that for the relevant transitions between the ground state and the one-exciton states and between the one-exciton states and the two-exciton states, Eq. (18) is equivalent to

$$M=RM_++M_-R. \tag{20}$$

Combining the above, one arrives at the absorption spectrum from state $|\mathrm{in}\rangle$ in terms of operators appropriate to the hard-core boson system:

$$I^{\mathrm{in}}(E)=-\pi^{-1}\,\mathrm{Im}\langle \mathrm{in}|M_-RG_{\mathrm{hcb}}(y_+)RM_+|\mathrm{in}\rangle +\pi^{-1}\,\mathrm{Im}\langle \mathrm{in}|RM_+G_{\mathrm{hcb}}(y_-)M_-R|\mathrm{in}\rangle. \tag{21}$$

Here, we used the fact that $G_{\mathrm{hcb}}(y_\pm)$ can contribute to the spectrum only if the dipole operator increases (for the upper sign) or decreases (for the lower sign) by one the number of excitons relative to the initial state.

Realizing that $RG_{\mathrm{hcb}}R=G_{\mathrm{hcb}}$ and $R|\mathrm{in}\rangle=|\mathrm{in}\rangle$, the projection operators may be dropped in Eq. (21), so that, after substituting Eq. (11), we obtain

$$I^{\mathrm{in}}(E)=I_0^{\mathrm{in}}(E)+\pi^{-1}\,\mathrm{Im}\langle \mathrm{in}|M_-G_0(y_+)\times(QG_0(y_+)Q)^{-1}G_0(y_+)M_+|\mathrm{in}\rangle, \tag{22}$$

with

$$I_0^{\mathrm{in}}(E)\equiv-\pi^{-1}\,\mathrm{Im}\langle \mathrm{in}|M_-G_0(y_+)M_+|\mathrm{in}\rangle +\pi^{-1}\,\mathrm{Im}\langle \mathrm{in}|M_+G_0(y_-)M_-|\mathrm{in}\rangle. \tag{23}$$

In deriving Eq. (22), we have used the fact that $M_-|\mathrm{in}\rangle\sim|g\rangle$, which is a physical state, so that $(QG_0Q)^{-1}G_0M_-|\mathrm{in}\rangle=0$.

It should now be noted that $I_0^{\mathrm{in}}(E)$ represents the absorption spectrum of a noninteracting boson system, starting from state $|\mathrm{in}\rangle$; the effect of the kinematic exciton–exciton interaction is fully contained in the second term of Eq. (22). As the noninteracting boson system is in fact a collection of harmonic oscillators, its absorption spectrum should not depend on the initial state (a harmonic oscillator only has linear response). To show this explicitly, it is useful to note that Eq. (23) can be rewritten as

$$I_0^{\mathrm{in}}(E)=\pi^{-1}\,\mathrm{Re}\int_0^\infty e^{i(E+i\eta)t}\times\langle \mathrm{in}|[M_-,(e^{-iH_0t}M_+e^{iH_0t})]_-|\mathrm{in}\rangle dt. \tag{24}$$

Because the operators $M_\pm$ are linear in Bose creation and annihilation operators and H_0 is a quadratic form in these operators, the commutator $[M_-,(e^{-iH_0t}M_+e^{iH_0t})]_-$ is a c-number. Thus, the right-hand side of Eq. (24) does not depend on the specific initial state, giving

$$I_0^{\mathrm{in}}(E)=I_0^g(E)=I^g(E). \tag{25}$$

Here, the last equality holds because the spectrum $I^g(E)$ only involves transitions between the ground state and the one-exciton states, for which the kinematic exciton–exciton interaction is ''switched off.''

If we now combine Eqs. (13), (22), and (25), we finally find for the differential absorption spectrum:

$$\Delta I^{\mathrm{in}}(E)=\pi^{-1}\,\mathrm{Im}\langle \mathrm{in}|M_-G_0(QG_0Q)^{-1}G_0M_+|\mathrm{in}\rangle \tag{26}$$

where the argument $y_+=E_{\mathrm{in}}+E$ has been omitted in the above Green operator G_0. Clearly, the entire pump–probe spectrum results from the scattering of the bosons on the hard-core potential. More generally, this scattering is responsible for all nonlinear optical response in the Frenkel exciton system.[40]

In the general case of a system that lacks translational symmetry, for instance due to energy disorder, the actual evaluation of Eq. (26) involves manipulating matrices of dimension $\mathcal{N}$ ($\mathcal{N}$ the number of molecules in the system). In particular, an $\mathcal{N}\times\mathcal{N}$ diagonalization is needed to find the one-boson energies occurring in G_0 and the matrix elements of M_+ and M_-. Furthermore, the evaluation of $(QG_0Q)^{-1}$ requires the inversion of another $\mathcal{N}\times\mathcal{N}$ matrix (for each energy E), as the space of doubly occupied states $(a_n^\dagger a_n^\dagger|g\rangle)$ has dimension $\mathcal{N}$. As was also pointed out by Mukamel and Leegwater,[40] this is an appreciable gain over a brute force calculation of the two-exciton states through diagonalization of H_{exc}, which involves matrices of dimension $\mathcal{N}(\mathcal{N}-1)/2$. For systems with translational symmetry, the $\mathcal{N}\times\mathcal{N}$ matrices involved in Eq. (26) can, too a large extent, even be handled analytically, as we will show in the next section.

As noted below Eq. (15), the differential absorption spectrum $\Delta I^{\mathrm{in}}(E)$ by construction has positive resonances if E equals the transition energy between the one-exciton $|\mathrm{in}\rangle$ and one of the states of the two-exciton band, while it has negative resonances at one-exciton energies. In our final result Eq. (26) the one-exciton resonances are contained in the

free-exciton Green operator G_0, while the middle factor $(QG_0Q)^{-1}$ (involving inversion of the projected Green operator) yields new resonances at the energies of one- to two-exciton transitions. We finally note that the above derivation of the differential absorption spectrum equally well holds if we keep η finite, which is a simple way of including a linewidth for all optical transitions.

IV. ORDERED SYSTEMS WITH SEVERAL DAVYDOV COMPONENTS

In this section, we consider aggregates which occupy a d-dimensional Bravais lattice consisting of N unit cells. Each unit cell contains S molecules, a situation which leads to the occurrence of S separate one-exciton bands (Davydov components).[1–3] The total number of molecules is thus $\mathcal{N}=NS$. It is now most convenient to replace the label n of the molecules by $\mathbf{n}s$, where $\mathbf{n}$ denotes the position vector of the unit cell to which the molecule belongs, while $s=1,\ldots,S$ specifies the molecules within each cell. We shall assume translational symmetry (i.e., absence of disorder), so that $\varepsilon_{\mathbf{n}s}=\varepsilon_s$ and $L_{\mathbf{n}s,\mathbf{n}'s'}=L_{s,s'}(\mathbf{n}-\mathbf{n}')$. Finally, we impose periodic boundary conditions on the Bravais lattice in the usual way.[45]

Under these conditions, the free-boson Hamiltonian H_0 of Eq. (5) can be diagonalized via the transformation:[1–3]

$$b^\dagger_{\mathbf{q}\sigma}=N^{-1/2}\sum_{\mathbf{n}s}\ \phi_{\sigma s}(\mathbf{q})\exp(i\mathbf{q}\cdot\mathbf{n})a^\dagger_{\mathbf{n}s}, \tag{27}$$

(and the hermitian conjugate for $b_{\mathbf{q}\sigma}$), the inverse transformation being given by

$$a^\dagger_{\mathbf{n}s}=N^{-1/2}\sum_{\mathbf{q}\sigma}\ \phi^*_{\sigma s}(\mathbf{q})\exp(-i\mathbf{q}\cdot\mathbf{n})b^\dagger_{\mathbf{q}\sigma}. \tag{28}$$

Here $b^\dagger_{\mathbf{q}\sigma}$ ($b_{\mathbf{q}\sigma}$) are the Bose operators for creation (annihilation) of an exciton in the σth Davydov band ($\sigma=1,\ldots,S$), and $\mathbf{q}$ denotes one of the N allowed wave vectors in the first Brillouin zone. Furthermore, $\phi_{\sigma s}(\mathbf{q})$ is the sth component of the σth eigenvector (normalized to unity) of the $S\times S$ matrix

$$H_{s,s'}(\mathbf{q})=\varepsilon_s\delta_{s,s'}+{\sum_{\mathbf{n}}}'\ L_{s,s'}(\mathbf{n})\exp(-i\mathbf{q}\cdot\mathbf{n}). \tag{29}$$

The corresponding set of eigenenergies will be denoted $E_{\mathbf{q}\sigma}$. The prime on the summation in Eq. (29) excludes the term with $\mathbf{n}=\mathbf{0}$ and simultaneously $s=s'$. After the above transformation, the Hamiltonian of Eq. (5) takes the diagonal form:

$$H_0=\sum_{\mathbf{q},\sigma}\ E_{\mathbf{q}\sigma}b^\dagger_{\mathbf{q}\sigma}b_{\mathbf{q}\sigma}. \tag{30}$$

On the new basis, the matrix elements of the Green operator G_0 ($=G_0(E_{\rm in}+E)$) in the subspace of two-exciton states are easily calculated to be

$$\langle g|b_{\mathbf{q}_1\sigma_1}b_{\mathbf{q}_2\sigma_2}G_0b^\dagger_{\mathbf{q}_3\sigma_3}b^\dagger_{\mathbf{q}_4\sigma_4}|g\rangle = \frac{\delta_{\mathbf{q}_1\sigma_1,\mathbf{q}_3\sigma_3}\delta_{\mathbf{q}_2\sigma_2,\mathbf{q}_4\sigma_4}+\delta_{\mathbf{q}_1\sigma_1,\mathbf{q}_4\sigma_4}\delta_{\mathbf{q}_2\sigma_2,\mathbf{q}_3\sigma_3}}{E+E_{\rm in}-E_{\mathbf{q}_3\sigma_3}-E_{\mathbf{q}_4\sigma_4}+i\eta}. \tag{31}$$

Furthermore, the dipole raising and lowering operators defined in Eq. (19) take the form

$$M_+=M_-^\dagger=\sum_{\mathbf{q}\sigma}\ \mu_{\mathbf{q}\sigma}b^\dagger_{\mathbf{q}\sigma}, \tag{32}$$

with

$$\mu_{\mathbf{q}\sigma}=N^{-1/2}\sum_{\mathbf{n}s}\ \mu_{\mathbf{n}s}\phi^*_{\sigma s}(\mathbf{q})\exp(-i\mathbf{q}\cdot\mathbf{n}). \tag{33}$$

Here, $\mu_{\mathbf{n}s}$ denotes the dipole matrix element of molecule $\mathbf{n}s$.

Finally, to evaluate the spectrum Eq. (26), we need the operator $(QG_0Q)^{-1}$. To this end, we first note that Eq. (9) for the projection operator Q (which also represents the hard-core interaction), may be written

$$Q=\frac{1}{2}\sum_{\mathbf{n}s}\ a^\dagger_{\mathbf{n}s}a^\dagger_{\mathbf{n}s}|g\rangle\langle g|a_{\mathbf{n}s}a_{\mathbf{n}s}=\sum_{\mathbf{K}s}\ B^\dagger_{\mathbf{K}s}|g\rangle\langle g|B_{\mathbf{K}s}, \tag{34}$$

where

$$B^\dagger_{\mathbf{K}s}\equiv(2N)^{-1/2}\sum_{\mathbf{k},\sigma,\sigma'}\ \phi^*_{\sigma s}(\mathbf{K}/2+\mathbf{k}) \times\phi^*_{\sigma' s}(\mathbf{K}/2-\mathbf{k})b^\dagger_{\mathbf{K}/2+\mathbf{k},\sigma}b^\dagger_{\mathbf{K}/2-\mathbf{k},\sigma'} \tag{35}$$

and the hermitian conjugate for $B_{\mathbf{K}s}$. The insertion of the projection operator $|g\rangle\langle g|$ is legitimate in Eq. (34), since we are dealing with states containing up to two excitons. Thus, the hard-core boson interaction has been expressed using auxiliary operators, $B^\dagger_{\mathbf{K}s}$ and $B_{\mathbf{K}s}$. These new operators describe, respectively, creation and annihilation of spatially extended unphysical boson pairs located at the same molecules of the type s and characterized by the center of mass momentum $\mathbf{K}$. The N allowed values for $\mathbf{K}$ are identical to those for $\mathbf{q}$ (the one-boson momenta), while the N allowed values for $\mathbf{k}$ are the same as those for $\mathbf{q}-\mathbf{K}/2$.

Using Eqs. (34), (35), and (31), one now easily arrives at

$$QG_0Q=\sum_{\mathbf{K},s,s'}\ D_{s,s'}(\mathbf{K})B^\dagger_{\mathbf{K}s}|g\rangle\langle g|B_{\mathbf{K}s'}, \tag{36}$$

where the $S\times S$ matrix $D_{s,s'}(\mathbf{K})$ is defined by

$$D_{s,s'}(\mathbf{K})=\frac{1}{N}\sum_{\mathbf{k},\sigma,\sigma'}\ \frac{\phi^*_{\sigma s}(\mathbf{K}/2+\mathbf{k})\phi_{\sigma s'}(\mathbf{K}/2+\mathbf{k})\phi^*_{\sigma' s}(\mathbf{K}/2-\mathbf{k})\phi_{\sigma' s'}(\mathbf{K}/2-\mathbf{k})}{E+E_{\mathbf{K}_0\sigma_0}-E_{\mathbf{K}/2+\mathbf{k},\sigma}-E_{\mathbf{K}/2-\mathbf{k},\sigma'}+i\eta}. \tag{37}$$

Here, we have assumed that when the probe pulse arrives, the system resides in the one-exciton state with momentum $\mathbf{K}_0$ in band σ_0,

$$|\mathrm{in}\rangle = b^{\dagger}_{\mathbf{K}_0\sigma_0}|g\rangle \equiv |\mathbf{K}_0\sigma_0\rangle, \tag{38}$$

characterized by the energy $E_{\mathrm{in}} = E_{\mathbf{K}_0\sigma_0}$. This ''initial state'' may result either directly from excitation by the pump pulse or from relaxation after this excitation. We note that the final result Eq. (40) is modified in a straightforward way if the initial state is an incoherent superposition of one-exciton states.

As the operators $B^{\dagger}_{\mathbf{K}s}$ produce an orthonormal set of two-boson states, $\langle g|B_{\mathbf{K}s}B^{\dagger}_{\mathbf{K}'s'}|g\rangle = \delta_{\mathbf{K}s,\mathbf{K}'s'}$, the operator QG_0Q can be inverted to yield [see remark below Eq. (12)]:

$$(QG_0Q)^{-1} = \sum_{\mathbf{K},s,s'} D^{-1}_{s,s'}(\mathbf{K}) B^{\dagger}_{\mathbf{K}s}|g\rangle\langle g|B_{\mathbf{K}s'}, \tag{39}$$

where $D^{-1}_{s,s'}(\mathbf{K})$ denotes the (s,s') component of the inverse of the matrix $D_{s,s'}(\mathbf{K})$.

We now have all ingredients to evaluate the differential absorption spectrum $\Delta I(E)$ given by Eq. (26). With the initial state Eq. (38) and using Eqs. (39), (35), (32), and (31), we arrive at (from now on we will drop the superscript referring to the initial state):

$$\Delta I(E) = \mathrm{Im}\frac{2}{\pi N}\sum_{\mathbf{q},s,s'} \tilde{f}_s(\mathbf{q}) D^{-1}_{s,s'}(\mathbf{K}_0+\mathbf{q}) f_{s'}(\mathbf{q}), \tag{40}$$

with

$$f_s(\mathbf{q}) = \sum_{\sigma} \frac{\mu_{\mathbf{q}\sigma}\phi_{\sigma_0 s}(\mathbf{K}_0)\phi_{\sigma s}(\mathbf{q})}{E - E_{\mathbf{q}\sigma} + i\eta} \tag{41}$$

and

$$\tilde{f}_s(\mathbf{q}) = \sum_{\sigma} \frac{\mu^*_{\mathbf{q}\sigma}\phi^*_{\sigma_0 s}(\mathbf{K}_0)\phi^*_{\sigma s}(\mathbf{q})}{E - E_{\mathbf{q}\sigma} + i\eta}. \tag{42}$$

Here the E-dependence is implicit in the quantities $D_{s,s'}(\mathbf{K}_0+\mathbf{q})$, $\tilde{f}_s(\mathbf{q})$, and $f_{s'}(\mathbf{q})$. As pointed out below Eq. (26), the original pump–probe spectrum involves the diagonalization of an $\mathcal{N}\times\mathcal{N}$ matrix and the inversion of another $\mathcal{N}\times\mathcal{N}$ matrix. By taking advantage of the translational symmetry, the problem has been reduced to the diagonalization of the $S\times S$ matrix $H_{s,s'}(\mathbf{q})$, which determines the eigenvectors $\phi_{\sigma s}(\mathbf{q})$ and eigenenergies $E_{\mathbf{q}\sigma}$. In addition, inversion of another $S\times S$ matrix $D_{s,s'}$ is needed to determine the pump–probe spectrum given by Eq. (40).

We conclude this section by presenting the results for the simple case of one molecule per unit cell ($S=1$). Then the indices s and σ become redundant and $\phi_{\sigma s}(\mathbf{q}) \equiv 1$, so that Eq. (40) reduces to

$$\Delta I(E) = \mathrm{Im}\frac{2}{\pi}\sum_{\mathbf{q}} \frac{|\mu_{\mathbf{q}}|^2}{(E - E_{\mathbf{q}} + i\eta)^2}\left[\sum_{\mathbf{k}} \frac{1}{E + E_{\mathbf{K}_0} - E_{(\mathbf{K}_0+\mathbf{q})/2+\mathbf{k}} - E_{(\mathbf{K}_0+\mathbf{q})/2-\mathbf{k}} + i\eta}\right]^{-1}, \tag{43}$$

with

$$E_{\mathbf{q}} \equiv \varepsilon + \sum_{\mathbf{n}\neq\mathbf{0}} L(\mathbf{n})\exp(-i\mathbf{q}\cdot\mathbf{n}) \tag{44}$$

and

$$\mu_{\mathbf{q}} = N^{-1/2}\sum_{\mathbf{n}} \mu_{\mathbf{n}}\exp(-i\mathbf{q}\cdot\mathbf{n}). \tag{45}$$

The values over which $\mathbf{q}$ and $\mathbf{k}$ run in the summations in Eq. (43) have been specified below Eqs. (28) and (35). We note that if all molecular transition dipoles are taken equal ($\mu_{\mathbf{n}} \equiv \mu$), we have $\mu_{\mathbf{q}} = \mu N^{1/2}\delta_{\mathbf{q},\mathbf{0}}$, so that the summation over $\mathbf{q}$ collapses to a single term. It is useful, however, to keep the more general form Eq. (43), in order to describe circular and cylindrical aggregates, in which the molecular dipoles rotate along with the position of the molecule on the curved structure.

V. ONE-DIMENSIONAL AGGREGATE WITH ONE MOLECULE PER UNIT CELL

In this section, we consider ordered one-dimensional aggregates with one molecule per unit cell. In this situation, the pump–probe spectrum is descibed by Eqs. (43)–(45) in which the wave vectors $\mathbf{k}$, $\mathbf{q}$, and $\mathbf{K}_0$ reduce to scalars k, q, and K_0. If we use the lattice constant as unit of length, the wave numbers q and K_0 can take the values $2\pi l_q/N$ and $2\pi l_0/N$, respectively, where l_q and l_0 both take the values $0,1,\ldots,N-1$. The allowed values for k also can be written as $k = 2\pi l_k/N$, but now $l_k = 0,1,\ldots,N-1$ if $l_q + l_0$ is even, whereas $l_k = \frac{1}{2},\frac{3}{2},\ldots,N-\frac{1}{2}$ if $l_q + l_0$ is odd.

For simplicity, we adopt the nearest-neighbor approximation, $L(n) = -L(\delta_{n,1} + \delta_{n,-1})$, giving

$$E_q = \varepsilon - 2L\cos q. \tag{46}$$

Using this dispersion relation, Eq. (43) reduces to

$$\Delta I(E) = -\frac{1}{2\pi L}\mathrm{Im}\sum_{q} \frac{|\mu_q|^2/N}{\cos(K/2)} \frac{[S_K(p)]^{-1}}{[p - \cos(K_0/2 - q/2)]^2}, \tag{47}$$

with $K \equiv K_0 + q$,

$$p = \frac{\varepsilon + 2L\cos K_0 - E - i\eta}{4L\cos(K/2)}, \tag{48}$$

and the function $S_K(z)$ defined through

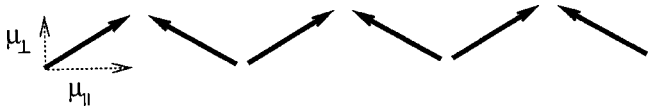

FIG. 1. Linear aggregate with alternating dipoles.

$$S_K(z)=\frac{1}{N}\sum_k \frac{1}{z-\cos k}. \tag{49}$$

Here, the dependence on K derives from the fact that the values taken by k in the right-hand-side summation depend on $K=K_0+q$ (see above). This summation can be evaluated analytically to yield:[46]

$$S_K(z)=\frac{2}{g(z)-g^{-1}(z)}\left(\frac{1+g^{-N}(z)e^{iKN/2}}{1-g^{-N}(z)e^{iKN/2}}\right)$$
$$=\frac{1}{z-1}\left(\frac{g(z)-1}{g(z)+1}\right)\left(\frac{1+g^{-N}(z)e^{iKN/2}}{1-g^{-N}(z)e^{iKN/2}}\right), \tag{50}$$

with $g(z)=z+\sqrt{z^2-1}$ and $g^{-1}(z)=z-\sqrt{z^2-1}$.

The specific form of the transition dipoles μ_q entering the line shape Eq. (47), depends on the geometry of the aggregate. Below we will consider two special examples for this geometry.

A. Chain with alternating dipoles

We first consider a linear molecular aggregate with alternating dipoles, as depicted in Fig. 1. Specifically, the molecular transition dipoles contain a constant component $\mu_\parallel$ along the aggregate axis and an alternating component $\mu_\perp(-1)^n$ perpendicular to it. The resulting transition dipoles of the aggregate are $\mu_q^\parallel=\delta_{q,0}\mu_\parallel\sqrt{N}$ and $\mu_q^\perp=\delta_{q,\pi}\mu_\perp\sqrt{N}$ for the electric field polarized parallel and perpendicular to the aggregate axis, respectively. Thus, for $L>0$, the ground-state absorption takes place to the bottom (top) of the one-exciton band for light that is polarized parallel (perpendicular) to the aggregate axis, and with corresponding strength $N\mu_\parallel^2(N\mu_\perp^2)$. This situation is believed to be realized in J aggregates of pseudo-isocyanine,[47,48] for which the $q=0$ transition (polarized along the aggregate axis) yields the narrow (zero-phonon) J band in the long-wavelength area of the spectrum, while the $q=\pi$ transition is responsible for the short-wavelength absorption of the aggregate in the perpendicular polarization.

Before proceeding with the pump–probe spectrum, we note that the structure depicted in Fig. 1 may equally well be considered an example of a system with two molecules per unit cell, with the $q=0$ and the $q=\pi$ transitions corresponding to the allowed transitions in the two different Davydov bands. From the point of view of the Hamiltonian (the energies and interactions), however, this separation into Davydov bands is not necessary, which is why we prefer to regard this as a system with one molecule per unit cell. Of course, the results do not depend on what point of view one takes, as long as the dipole orientations are properly taken into account.

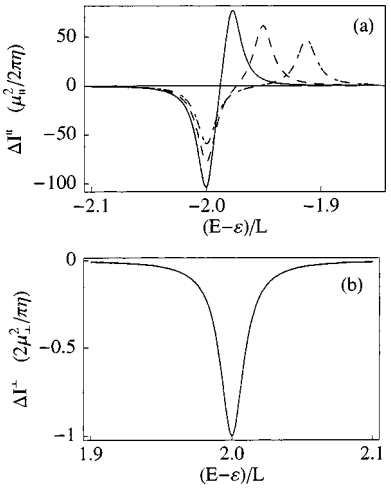

FIG. 2. (a) Differential absorption spectrum according to Eq. (51) for a linear chain of alternating dipoles probed with light polarized parallel to the chain direction and starting from an initial condition with wave number $K_0=0$. The three different spectra correspond to chain sizes $N=15$ (dashed–dotted), 20 (dashed), and 30 (solid), respectively. In all cases the linewidth was set to $\eta=0.01L$. (b) As in (a) but now for a probe pulse polarized perpendicular to the chain direction [Eq. (52)]. The spectrum then does not depend on the size of the chain.

Let us now suppose that in the pump–probe experiment the aggregate resides in the $|K_0=0\rangle$ one-exciton state when the probe arrives (for instance due to using a pump pulse with parallel polarization). Then Eq. (47) yields the following differential absorption spectra for the probe pulse polarized parallel and perpendicular to the aggregate axis, respectively,

$$\Delta I^\parallel(E)=-\frac{|\mu_\parallel|^2}{2\pi L}\mathrm{Im}\frac{1}{p-1}\left(\frac{g(p)+1}{g(p)-1}\right)\left(\frac{1-g^{-N}(p)}{1+g^{-N}(p)}\right), \tag{51}$$

[p as in Eq. (48) with $K=K_0=0$] and

$$\Delta I^\perp(E)=\frac{2|\mu_\perp|^2}{\pi}\mathrm{Im}\frac{1}{E-\varepsilon-2L+i\eta}. \tag{52}$$

Equation (52) may be derived by taking the limit $q\to\pi$ in Eq. (47) or, alternatively, directly from Eq. (43) by noting that for $q=\pi$ the summation over k is trivial, as then the summand does not depend on k.

The above result for $\Delta I^\parallel(E)$ agrees with the line shape obtained if one uses the Jordan–Wigner transformation to transform the original paulions to fermions [cf. Eq. (4.3) of Ref. 11].[49] As is seen in Fig. 2(a), this line shape exhibits, in addition to the one-exciton bleaching peak, the well-known blueshifted induced-absorption peak characteristic of the J band (Sec. I). For η small enough, the intensities of the bleaching and induced-absorption peaks scale proportional to N, due to the superradiant nature of the corresponding transitions. Figure 2(a) also clearly displays the sensitivity of the blueshift of the induced absorption to the size of the aggregate. On the other hand, in the limit of large aggregates ($N\gg\sqrt{3\pi^2L/\eta}$), the differential absorption spectrum becomes size independent.[8,50] This is clear from the fact that for large

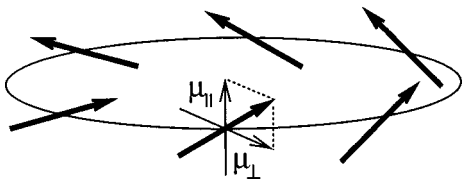

FIG. 3. Ring aggregate with the molecular dipoles indicated by the thick arrows. The projection of the dipoles along the direction perpendicular to the plane of the ring has magnitude $\mu_\parallel$, while the projection on the plane of the ring has magnitude $\mu_\perp$.

N the last factor in Eq. (51) approaches 1 [if $g(p)>1$] or -1 [if $g(p)<1$]. We finally note that the spectrum obeys the sum-rule:[4]

$$\int \Delta I^{\parallel}(E)dE = -2|\mu_\parallel|^2, \tag{53}$$

which is independent of the strength L of the transfer interaction and would also hold in the presence of disorder and (or) exciton-phonon coupling.

In contrast to the ''parallel'' spectrum, its perpendicular counterpart $\Delta I^{\perp}(E)$ only displays a single Lorenztian bleaching peak, which is centered at the top of the one-exciton band [Fig. 2(b)]. The intensity of the bleaching peak does not depend on N. This agrees with the sum-rule Eq. (53), which is obeyed by $\Delta I^{\perp}(E)$ as well, except that $\mu_\parallel$ is replaced by $\mu_\perp$. The explanation why $\Delta I^{\perp}(E)$ only has a single bleaching peak and does not exhibit the common dispersive shape characteristic of J-aggregates, lies in the strong degeneracy of the two-exciton states of interest. This is best understood using the fermion picture resulting from the Jordan–Wigner transformation (this method can be applied in the present special case of one dimension and nearest-neighbor interaction). In the fermion picture, the induced-absorption resonances occur at $E=E_{k_1}+E_{\pi-k_1}-E_{K_0=0}$, where we used the selection rule $K_0=k_1+k_2-\pi$, which is appropriate for excitation with light of perpendicular polarization (k_1 and k_2 are fermion wave numbers). Using Eq. (46), one finds that the quantity $E_{k_1}+E_{\pi-k_1}=2\varepsilon$ is independent of k_1. Consequently, all induced-absorption contributions with perpendicular polarization take place at $E=\varepsilon+2L$, which is in exact resonance with the only one-exciton bleaching peak that is visible in perpendicular polarization. This explains why only a single net bleaching feature is observed. We note that in our hard-core boson approach the degeneracy of many bleaching and induced-absorption peaks can be seen by comparing the various k contributions in Eq. (43) with $q=\pi$ and $K_0=0$.

B. Ring aggregate

Next we consider aggregates with a circular geometry (Fig. 3), as is realized in bacterial antenna complexes.[51] The molecular transition dipoles have a constant component $\mu_z=\mu_\parallel$ parallel to the aggregate axis and a component $\mu_\perp$ lying in the plane of the ring and rotating perpendicular to the axis. Arbitrarily assigning the x direction to the in-plane dipole component belonging to molecule $n=0$ and the y direction perpendicular to it, we have $\mu_{n,x}=\mu_\perp\cos(q_0 n)$ and $\mu_{n,y}=\mu_\perp\sin(q_0 n)$, with $q_0=2\pi/N$.

For electric fields polarized parallel to the aggregate axis, the transition dipoles of the total aggregate are now given by $\mu_q^{\parallel}=\delta_{q,0}\mu_\parallel\sqrt{N}$. For electric fields polarized perpendicular to the aggregate axis, we have

$$\mu_{q,x}=(\delta_{q,q_0}+\delta_{q,-q_0})\frac{\mu_\perp}{2}\sqrt{N},$$

$$\mu_{q,y}=(\delta_{q,q_0}-\delta_{q,-q_0})\frac{\mu_\perp}{2i}\sqrt{N}. \tag{54}$$

Consequently, the optically allowed transitions from the ground state take place to the one-exciton states with $q=0$ (parallel polarization) or $q=\pm q_0$ (perpendicular polarization). The latter two states are degenerate.

If the aggregate resides in the one-exciton state with $K_0=0$ when the probe pulse arrives, the differential spectrum in parallel polarization is once again given by Eq. (51). This is not surprising, as light of this polarization only ''sees'' the molecular dipole components perpendicular to the plane of the ring, which are all identical. Thus, the ring becomes equivalent to a linear chain with periodic boundary conditions and with all molecular dipoles parallel to each other. This indeed is exactly the situation in the previous subsection, provided we probe the chain with parallel polarization. In view of this equivalence, we will not analyze this spectrum in more detail.

On the other hand, if we use a probe pulse with perpendicular polarization, the situation is drastically different from the linear chain with alternating dipoles. This is due to the fact that in the ring light of this polarization probes the component of the molecular dipole that rotates around the ring axis (wave numbers $\pm q_0$), while in the linear chain of the previous subsection, it probes the alternating component of the dipole (wave vector π). Using Eqs. (47) and (54), we find

$$\Delta I^x(E)=\Delta I^y(E)$$
$$=-\frac{|\mu_\perp|^2}{4\pi L}\,\mathrm{Im}\,\frac{1}{\cos(\pi/N)}\,\frac{p-1}{[p-\cos(\pi/N)]^2}$$
$$\times\left(\frac{g(p)+1}{g(p)-1}\right)\left(\frac{1+g^{-N}(p)}{1-g^{-N}(p)}\right), \tag{55}$$

where p is taken from Eq. (48) with $K_0=0$ and $K=\pm q_0$. Without showing figures, we note that these perpendicular spectra are again of the familiar dispersive shape [cf. Fig. 2(a)], except that (for $L>0$) the entire spectrum is blue-shifted compared to the spectrum Eq. (51), while also the spectral separation between the bleaching and the induced absorption is increased. This is due to the change in selection rules. However, one easily checks that in the limit of large N, the spectrum Eq. (55) becomes identical to Eq. (51) (with $\mu_\parallel$ replaced by $\mu_\perp$). This is understood from the fact that in this limit the curvature of the ring is not important anymore on

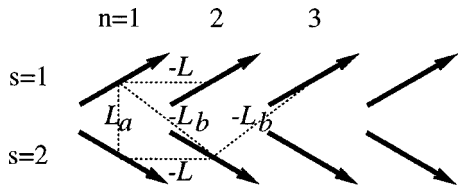

FIG. 4. One-dimensional aggregate with a herringbone structure. The arrows indicate the molecular transition dipoles. Also indicated are the three different types of transfer interactions that are taken into account.

the scale of the coherence length $\sqrt{3\pi^2 L/\eta}$. We finally note that the spectra Eq. (55) obey the sumrule $\int[\Delta I^x(E)+\Delta I^y(E)]dE=-2|\mu_\perp|^2$.

VI. LINEAR AGGREGATE WITH HERRINGBONE STRUCTURE

We next consider linear aggregates with two molecules per unit cell. The studied structure is of the herringbone type, depicted in Fig. 4, in which the unit cell contains two identical molecules ($s=1$ and $s=2$), which only differ in the orientation of their transition dipoles. The latter all have identical components $\mu_\parallel$ along the aggregate axis and a component $\mu_\perp(-1)^{s+1}$ perpendicular to it. We assume the following nonzero transfer interactions: $L_{ns,(n+1)s}\equiv -L$, $L_{n1,n2}\equiv L_a$, $L_{n1,(n+1)2}=L_{(n+1)1,n2}\equiv -L_b$, together with the hermitian conjugated contributions. Here the signs have been chosen to make the quantities L, L_a, and L_b positive if the dipole–dipole coupling dominates and the dipoles are oriented relatively close to the aggregate axis. If the interactions are assumed real, the matrix Eq. (29) takes the form:

$$H_{s,s'}(q)=(\varepsilon-2L\cos q)\delta_{s,s'}+(L_a-2L_b\cos q)(1-\delta_{s,s'}), \tag{56}$$

where ε is the molecular transition energy, which is equal for both molecules. The one-exciton wave number q takes the same values as in Sec. V. For each q, $H_{s,s'}(q)$ represents a 2×2 matrix, which is easily diagonalized to yield

$$E_{q\sigma}=\varepsilon-2L\cos q+\sigma(L_a-2L_b\cos q) \tag{57}$$

and

$$\phi_{\sigma s}=(\sigma)^{s+1}/\sqrt{2}, \tag{58}$$

with $\sigma=\pm 1$ labeling the two dispersion branches. It is noteworthy that the eigenvectors Eq. (58) are independent of q. This considerably simplifies the following analysis.

We now turn to the transition dipoles of the aggregate. For the electric field polarized along the chain, one has

$$\mu^{\parallel}_{q\sigma}=\mu_\parallel\sqrt{2N}\,\delta_{q,0}\delta_{\sigma,1}, \tag{59}$$

so that the ground-state absorption exhibits a peak at $E_{0,+1}=\varepsilon-2L+L_a-2L_b$ with strength $2N\mu_\parallel^2$. On the other hand, for the electric field polarized perpendicular to the chain the transition dipoles read:

$$\mu^{\perp}_{q\sigma}=\mu_\perp\sqrt{2N}\,\delta_{q,0}\delta_{\sigma,-1}, \tag{60}$$

giving a ground-state absorption of strength $2N\mu_\perp^2$ and positioned at $E_{0,-1}=\varepsilon-2L-L_a+2L_b$. Thus, provided that $L_a-2L_b\neq 0$, a Davydov splitting is observed between the absorption lines with different polarizations.

The technical steps needed to derive from Eq. (40) the differential absorption spectra for parallel and perpendicular probe polarization are outlined in Appendix C. Here, we only quote the results obtained if one assumes that at the moment that the probe pulse arrives, the aggregate resides in the one-exciton state with wave number $\mathbf{K}_0=0$ and branch label $\sigma_0=+1$. This state may be created by using a pump that is polarized parallel to the chain. Following the steps in Appendix C, one arrives at

$$\Delta I^{\parallel}(E)=\mathrm{Im}\frac{2}{\pi}\frac{\mu_\parallel^2}{(E-E_{0,+1}+i\eta)^2}\left(\sum_{\sigma=\pm 1}\frac{1}{8(L+\sigma L_b)}\frac{1}{(p_\sigma-1)}\frac{1-g(p_\sigma)}{1+g(p_\sigma)}\frac{1+g^{-N}(p_\sigma)}{1-g^{-N}(p_\sigma)}\right)^{-1} \tag{61}$$

and

$$\Delta I^{\perp}(E)=\mathrm{Im}\frac{8L}{\pi}\frac{\mu_\perp^2(p_0-1)}{(E-E_{0,-1}+i\eta)^2}\frac{1+g(p_0)}{1-g(p_0)}\frac{1-g^{-N}(p_0)}{1+g^{-N}(p_0)}. \tag{62}$$

Here the function g has been defined below Eq. (50), while

$$p_\alpha\equiv\frac{\varepsilon+2L-L_a(1-2\alpha)+2L_b-E-i\eta}{4(L+\alpha L_b)}, \tag{63}$$

with $\alpha=0,\pm 1$.

One easily checks that for $L_a=L_b=0$, Eq. (61) reduces to Eq. (51), while Eq. (62) reduces to Eq. (51) with $\mu_\parallel$ replaced by $\mu_\perp$. This should be expected, as in this limit the herringbone structure falls apart into two noninteracting linear aggregates with all dipoles oriented in the same direction. Light of parallel (perpendicular) polarization will then probe the parallel (perpendicular) components of the molecular dipoles only.[52] A second limiting case of interest is $L=L_b=0$, where the aggregate reduces to a collection of noninteracting dimers. It is easily verified that in this limit the above general spectra indeed yield the dimer spectra, which can be calculated in a straightforward way due to the small number of one-exciton states (2) and two-exciton states (1) that occur in a dimer.

Away from these limiting cases, the spectra show a richer variety of structures, depending on the relative position of the two Davydov bands. From Eq. (57) one finds that for $L_a-2L_b<0$ ($L_a-2L_b>0$) the bottom of the $\sigma=+1$ band lies lower (higher) than the bottom of the $\sigma=-1$ band (we assume $L>|L_b|$). Since in bleaching one observes only the $\sigma=+1$ band in parallel polarization and the $\sigma=-1$ band in perpendicular polarization, one thus expects that the

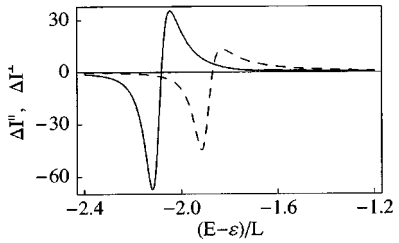

FIG. 5. Differential absorption spectrum for a linear chain with a herringbone structure (Fig. 4), taking as initial condition when the probe pulse arrives the one-exciton state with wave number $K_0=0$ residing in the Davydov branch $\sigma_0=+1$. The solid line reflects the spectrum for a probe pulse polarized parallel to the chain direction, while the dashed line corresponds to a probe with perpendicular polarization. The spectra have been calculated from Eqs. (61) and (62), using $L_a=0.5L$ and $L_b=0.3L$ for the interactions, $\eta=0.05L$ for the line width, and $N=1000$ for the chain size. The units of absorption used along the vertical axis are $\mu_{\|}^2/2\pi\eta$ and $\mu_{\perp}^2/2\pi\eta$ for $\Delta I^{\|}$ and $\Delta I^{\perp}$, respectively.

bleaching in parallel polarization occurs at lower (higher) frequency than the one in perpendicular polarization if $L_a-2L_b<0$ $(L_a-2L_b>0)$. This is indeed reflected in the spectra displayed in Figs. 5 and 6. These figures also clearly show that, again, the induced-absorption contributions occur mainly on the high-energy side of the bleaching peaks.

Interestingly, however, we observe some induced absorption to the low-energy side of the bleaching peak in the parallel spectrum of Fig. 6. This is related to the fact that the initial state ($|K_0=0,\sigma_0=+1\rangle$) is not the lowest one-exciton state, as the bottom of the $\sigma=-1$ band lies lower for the parameter values considered $(L_a-2L_b>0)$. As a consequence, if the probe excites an additional exciton in the $\sigma=-1$ band, this may result in induced-absorption features below the initial state. Since in the case of the parallel spectrum the bleaching occurs at the energy of the initial state, this immediately explains why induced-absorption contributions occur to the red of the bleaching peak. These contributions are weak (as observed), because they depend on the mixing of the two Davydov bands due to the kinematic interaction between excitons. If it were not for this interaction, the lower one- to two-exciton transition originating from the $\sigma=-1$ band would not be observable in parallel polarization. Therefore, the dominant induced-absorption features still occur blueshifted compared to the bleaching, as is commonly the case for exciton bands which have their bottom at $q=0$. We finally note that in perpendicular polarization no redshifted induced absorption features occur, as in this polarization the bleaching really occurs at the lowest possible one-exciton state.

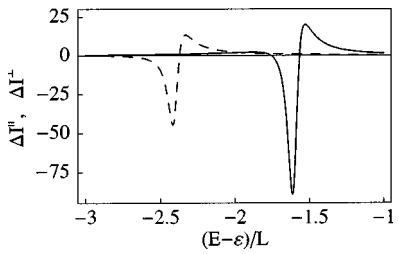

FIG. 6. As Fig. 5, but now with $L_a=L$, all other parameters unchanged.

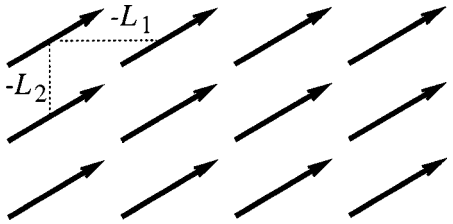

FIG. 7. Two-dimensional aggregate with one molecule per unit cell. The arrows indicate the molecular transition dipoles. Also indicated are the two nearest-neighbor transfer interactions that are taken into account in our explicit calculations.

VII. MONOLAYER WITH ONE MOLECULE PER UNIT CELL

As final example, we consider a two-dimensional square lattice of size $N_1\times N_2$ with one molecule per unit cell (Fig. 7), so that we may use Eq. (43) for the pump–probe spectrum. We will assume nearest-neighbor transfer interactions $-L_1$ in one of the lattice directions and $-L_2$ in the other direction. Then the one-exciton energies Eq. (44) take the form

$$E_{\mathbf{q}}=\varepsilon-2L_1\cos q_1-2L_2\cos q_2, \tag{64}$$

where $q_1=2\pi l_1/N_1$ and $q_2=2\pi l_2/N_2$ are the two components of the wavevector in units of the inverse lattice constant ($l_1=0,1,\ldots,N_1-1$; $l_2=0,1,\ldots,N_2-1$). Moreover, as we take all molecular transition dipoles equal (magnitude μ in the direction of the probe polarization), we have $\mu_{\mathbf{q}}=\mu N^{1/2}\delta_{\mathbf{q},\mathbf{0}}$, with $N=N_1N_2$. Substituting these results into Eq. (43) and denoting the wave vector of the initial state as $\mathbf{K}_0=(K_1,K_2)$, one finds

$$\Delta I(E)=\frac{\mu^2}{\pi}\,\mathrm{Im}\,\frac{2}{(E-\varepsilon+2L_1+2L_2+i\eta)^2}\times\left[\frac{1}{N}\sum_{k_1,k_2}\frac{1}{E-\varepsilon-L_1h(K_1,k_1)-L_2h(K_2,k_2)+i\eta}\right]^{-1}, \tag{65}$$

with

$$h(K_i,k_i)=2\cos K_i-4\cos(K_i/2)\cos k_i. \tag{66}$$

The allowed values for the wave vector components k_1 and k_2 depend on K_1 and K_2, respectively, similar as discussed in Sec. V for the wave numbers in the one-dimensional case.

The nature of the monolayer depends on the signs of L_1 and L_2. If both are positive, the optically allowed state $|\mathbf{q}=\mathbf{0}\rangle$ is the lowest one-exciton and the monolayer then behaves as a J aggregate. It is more common, however, that one of the interactions is positive, while the other is negative (the J–H aggregate). This situtation arises if the transfer interaction is of dipolar nature and the molecular dipoles lie in the plane of the monolayer. For explicitness we will from now on assume that $L_1>0$, while $L_2<0$. In that case, the lowest one-exciton state is optically forbidden and has wave vector $(0,\pi)$, while the optically allowed state with wave vector $(0,0)$ lies in a saddlepoint of the two-dimensional exciton dispersion manifold.

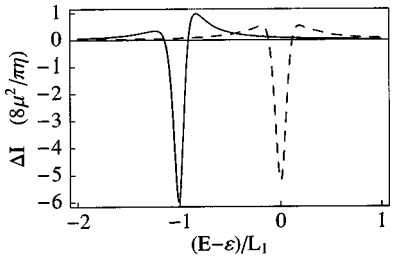

FIG. 8. Differential absorption spectrum for a monolayer (Fig. 7), taking as initial condition when the probe pulse arrives the optically allowed one-exciton state with wave vector $\mathbf{K}_0=(0,0)$, created by the pump pulse. The spectrum has been calculated using Eq. (68). The solid line corresponds to the case $L_2=-0.5L_1$, while the dashed line represents the case $L_2=-L_1$. In both cases the line width was set to $\eta=0.1L_1$, while the system size was taken $N_1\times N_2=100\times 100$ molecules.

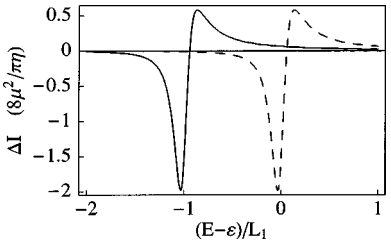

FIG. 9. As Fig. 8, but now assuming that by the time the probe pulse arrives, the system has relaxed to the lowest one-exciton state, i.e., the state with wave vector $\mathbf{K}_0=(0,\pi)$. All other parameters as in Fig. 8.

We will first consider the differential absorption spectrum assuming that when the probe pulse arrives the monolayer is in the state $|(K_1,K_2)\rangle=|(0,0)\rangle$. This represents the situation where the delay time between pump and probe is short enough to neglect relaxation of the optically allowed one-exciton state created by the pump–pulse to lower one-exciton states. With this initial condition, k_1 and k_2 in Eq. (65) take the same values as q_1 and q_2, respectively, specified below Eq. (64). After introducing

$$p_{k_2}=\frac{\varepsilon+2L_1+2L_2-4L_2\cos k_2-E-i\eta}{4L_1}, \tag{67}$$

the summation over k_1 may be performed by using an analog of Eq. (50), leading to

$$\Delta I(E)=\frac{\mu^2}{\pi}\,\mathrm{Im}\,\frac{8L_1}{(E-\varepsilon+2L_1+2L_2+i\eta)^2}\times\left[\frac{1}{N_2}\sum_{k_2}\frac{1}{(p_{k_2}-1)}\,\frac{1-g(p_{k_2})}{1+g(p_{k_2})}\,\frac{1+g^{-N_1}(p_{k_2})}{1-g^{-N_1}(p_{k_2})}\right]^{-1}, \tag{68}$$

with the function g as defined below Eq. (50).

Figure 8 displays the resulting spectrum for two different values of $|L_2/L_1|$ in the limit of a large monolayer, where the spectrum has become size-independent. The most interesting feature in these spectra is that the induced absorption occurs both on the high- and the low-energy side of the bleaching peak. As in Sec. VI (Fig. 6) this is a consequence of the fact that the initial state is not the lowest one-exciton state. As the ratio $|L_2/L_1|$ determines how much the lowest one-exciton state lies below the initial state, one expects that the amount of redshifted induced absorption grows at the expense of blueshifted induced absorption with growing $|L_2/L_1|$. This is indeed observed in Fig. 8.

We now turn to the other extreme situation, where the pump–probe delay time is long enough and the temperature low enough to assume that the optically pumped state has relaxed completely to the lowest one-exciton state. Thus, the initial state when the probe pulse arrives is $|(K_1,K_2)\rangle=|(0,\pi)\rangle$. Then the function $h(K_2,k_2)$ occurring in Eq. (65) becomes a constant $[h(\pi,k_2)=-2]$, so that the summand is independent of k_2. This immediately reduces the summation to a single one (over k_1, taking the same values as q_1 above), which may be carried out in analogy to Sec. V. The final result is identical to the spectrum Eq. (51), except that we should replace: $\mu_\parallel\to\mu$, $L\to L_1$, $N\to N_1$, and $E\to E+2L_2$. Thus, the spectrum for the monolayer under these conditions is given by a shifted version of the parallel spectrum for the chain with alternating dipoles. In particular, this implies that after relaxation to the lowest one-exciton state the spectrum, not surprisingly, only exhibits induced-absorption contributions on the blue side of the bleaching peak. Figure 9 displays the resulting spectrum for the same parameter values as used in Fig. 8.

Comparing Figs. 8 and 9, it is clear that relaxation through the one-exciton band has a strong influence on the shape of the pump–probe spectrum. Unravelling the resulting (ultrafast) time dependence of this spectrum in more detail involves a microscopic exciton–phonon coupling model.[53] Such a study, interesting as it may be, lies outside the scope of the current paper.

VIII. CONCLUDING REMARKS

In this paper, we have studied the pump–probe spectrum of Frenkel excitons in molecular assemblies with arbitrary structure and dimension. Our method is based on the hard-core boson approach, in which the paulions (excitons) are replaced by bosons with an infinite on-site repulsion. We have justified this method rigorously by using the Agranovich–Toshich transformation from paulions to bosons. Using the thus obtained two-exciton Green function, we have derived a general expression for the differential pump–probe spectrum [Eq. (26)]. Although this general result does not assume translational invariance (and thus also holds in the case of disorder), in our detailed analysis we have focused on ordered systems occupying a lattice. In particular, we have allowed for lattices containing more than one molecule per unit cell, thus giving rise to different Davydov components. The resulting spectrum Eq. (40) only involves the diagonalization and inversion of $S\times S$ matrices, where S is the number of molecules per unit cell. While it is well-known that disorder often plays an important role in molecular assemblies, it also is well-appreciated that semi-analytical spectra derived for ordered aggregates are useful to understand the salient spectral features observed in experiments. We hope that the explicit expressions presented by us for various types of aggregates will serve this purpose.

As specific applications, we have considered the linear chain with alternating dipoles, the ring aggregate, the chain with herringbone structure (two molecules per unit cell), and the monolayer. From these examples we have seen that the differential absorption spectrum exhibits a variety of shapes, depending on the structure of the assembly, the interaction parameters, and the polarization of the probe pulse. For a chain of alternating dipoles (as is believed to be a relevant model for PIC *J* aggregates), the differential absorption spectrum probed with parallel polarization contains a one- to two-exciton induced absorption peak that is blueshifted compared to the one-exciton bleaching peak [Fig. 2(a)]. On the other hand, perpendicular polarization only exhibits a small bleaching feature as a resultant of overlapping bleaching and induced-absorption contributions [Fig. 2(b)]. A different type of behavior is observed in systems with several Davydov branches or with a higher dimensional exciton dispersion manifold. In such systems, induced-absorption peaks can be observed simultaneously on the red and the blue side of the bleaching and stimulated emission peak (Figs. 6 and 8). This is analogous to the observation of positive two-photon absorption contributions on both sides of the one-exciton bleaching peak in the cw nonlinear absorption spectrum calculated by Leegwater and Mukamel.[40] In the pump–probe spectrum this phenomenon is dynamic and will, as a consequence of relaxation, evolve to the generic *J* aggregate differential absorption spectrum with growing pump–probe delay time (Figs. 8 and 9). These changes most likely take place on an ultrashort (femtosecond) time scale and may yield interesting information on the exciton–phonon coupling.

As discussed in Sec. II, the pump–probe signal which we derived originates from the kinematic interaction between the excitons, which reflects the Pauli exclusion for double excitation of a single two-level molecule. Alternative contributions to the nonlinear response arise from dynamic exciton–exciton interactions (quartic terms in the Hamiltonian),[2,3] which may lead to the formation of bound biexciton states. Although the effect of such interactions on the pump–probe spectrum has been considered theoretically,[8,11,54] to date no experimental signature of bound states in molecular assemblies has been reported.

We finally note that in a forthcoming paper we will analyze the differential absorption spectrum of cylindrical molecular structures, which have been observed for a class of substituted cyanine dyes.[35,36]

ACKNOWLEDGMENTS

We thank Professor P. Reineker and L. D. Bakalis for helpful discussions. One of us (G.J.) wishes to thank the Alexander von Humboldt Foundation for support. Also support from the Material Science Center of the University of Groningen is acknowledged.

APPENDIX A: JUSTIFICATION OF THE HARD-CORE BOSON APPROACH

In this appendix, we give a rigorous justification of the hard-core boson approach. Using Eqs. (4), (8), and (9) one finds

$$H_{\mathrm{hcb}}=H_{\mathrm{exc}}-V_{\mathrm{kin}}+\frac{A}{2}\sum_n a_n^\dagger a_n^\dagger a_n a_n . \tag{A1}$$

Upon substitution of Eq. (6) for V_{kin}, this yields

$$H_{\mathrm{hcb}}=H_0'+V, \tag{A2}$$

with

$$H_0'=H_{\mathrm{exc}}+\sum_n \left(\frac{A}{2}+\varepsilon_n\right) a_n^\dagger a_n^\dagger a_n a_n , \tag{A3}$$

and

$$V=\sum_{n\neq n'} L_{n,n'}(a_n^\dagger a_n^\dagger a_n a_{n'}+a_n^\dagger a_{n'}^\dagger a_{n'} a_{n'}). \tag{A4}$$

Thus, the zero-order Hamiltonian H_0' has been chosen to contain the full original Hamiltonian H_{exc} plus the unphysical part $\Sigma_n(A/2+\varepsilon_n)a_n^\dagger a_n^\dagger a_n a_n$.

If we now define the Green operators corresponding to H_{hcb} and H_0', respectively, as

$$G_{\mathrm{hcb}}\equiv(x-H_{\mathrm{hcb}}+i\eta)^{-1} \quad \text{and} \quad G_0'\equiv(x-H_0'+i\eta)^{-1}, \tag{A5}$$

iteration of the Dyson equation for G yields

$$G_{\mathrm{hcb}}=G_0'+G_0'VG_0'+G_0'VG_0'VG_0'+\cdots . \tag{A6}$$

Since $H_{\mathrm{exc}}a_n^\dagger a_n^\dagger|g\rangle\equiv 0$, the Hamiltonian H_0' contains no interaction between the physical and unphysical states. Consequently, the zero-order Green operator G_0' can be separated into physical and unphysical parts as

$$G_0'\equiv RG_0'R+QG_0'Q=(xR-H_{\mathrm{exc}})^{-1} + \left[xQ-\sum_n \left(\frac{A}{2}+\varepsilon_n\right) a_n^\dagger a_n^\dagger a_n a_n\right]^{-1}, \tag{A7}$$

where R denotes the operator for projection on the subspace of physical states [$R=I-Q$, I the unit operator and Q as defined in Eq. (9)]. Since $A\to\pm\infty$, the unphysical part in the above expression tends to zero for finite values of x, giving

$$G_0'=(xR-H_{\mathrm{exc}}+i\eta)^{-1}=G_{\mathrm{exc}}, \tag{A8}$$

with G_{exc} the Green operator Eq. (7) of the original paulion Hamiltonian.

We next note that the interaction operator V has matrix elements only between physical and unphysical states, so that

$$G_0'VG_0'=0. \tag{A9}$$

Combining Eqs. (A6), (A8), and (A9), one arrives at Eq. (10), i.e., the exact equivalence of the Green operators G_{exc} and G_{hcb} corresponding to the original Hamiltonian H_{exc} and the hard-core Hamiltonian H_{hcb}, respectively, within the subspace of one- and two-exciton states.

APPENDIX B: GREEN OPERATOR FOR THE HARD-CORE HAMILTONIAN

In this appendix, we solve the two-particle Green function for the hard-core boson model. Using Eq. (8), the Dyson equation for G reads

$$G_{\mathrm{hcb}}=G_0+AG_0QG_{\mathrm{hcb}} \quad \text{with } A\to\pm\infty \tag{B1}$$

or

$$QG_{\mathrm{hcb}}=QG_0+AQG_0QG_{\mathrm{hcb}}. \tag{B2}$$

This yields

$$(Q-AQG_0Q)QG_{\mathrm{hcb}}=QG_0 \tag{B3}$$

or, equivalently,

$$QG_{\mathrm{hcb}}=(Q-AQG_0Q)^{-1}QG_0. \tag{B4}$$

Substituting Eq. (B4) into Eq. (B1), one has

$$G_{\mathrm{hcb}}=G_0+AG_0Q(Q-AQG_0Q)^{-1}QG_0, \tag{B5}$$

which for $A\to\pm\infty$ reduces to Eq. (11) of the main text.

APPENDIX C: DERIVATION OF EQS. (61) AND (62)

The quantities $f_s(q)=\tilde{f}_s(q)$ entering the differential spectrum Eq. (40), depend on the polarization of the probe pulse. Substituting Eqs. (58)–(60) into Eq. (41), one finds

$$f_s^{\parallel}(q)=\sqrt{\frac{N}{2}}\frac{\mu_{\parallel}(\sigma_0)^{s+1}}{E-E_{q,+1}+i\eta}\delta_{q,0} \tag{C1}$$

and

$$f_s^{\perp}(q)=\sqrt{\frac{N}{2}}\frac{\mu_{\perp}(\sigma_0)^{s+1}(-1)^{s+1}}{E-E_{q,-1}+i\eta}\delta_{q,0} \tag{C2}$$

for the parallel and perpendicular polarizations, respectively. To determine the pump–probe spectrum, the matrix $D_{s,s'}(K_0+q)$ is now to be inverted. Substituting Eq.(58) into Eq. (37), one finds for $q=0$:

$$D_{s,s'}\equiv D_{s,s'}(K_0)=\frac{1}{4N}\sum_{k,\sigma,\sigma'}\frac{(\sigma)^{s+s'}(\sigma')^{s+s'}}{E+E_{K_0\sigma_0}-E_{K_0/2+k,\sigma}-E_{K_0/2-k,\sigma'}+i\eta}, \tag{C3}$$

with the allowed k values determined by K_0 as explained in Sec. V. From Eq. (37) it is clear that $D_{1,1}=D_{2,2}$ and $D_{1,2}=D_{2,1}$, so that

$$D_{s,s'}^{-1}=(D_{1,1}^2-D_{1,2}^2)^{-1}D_{s,s'}(-1)^{s+s'}. \tag{C4}$$

Substituting Eqs. (C1), (C2), and (C4) into Eq. (40), one arrives after straightforward algebra at the differential spectra for both probe polarizations:

$$\Delta I^{\parallel}(E)=\mathrm{Im}\frac{2}{\pi}\frac{\mu_{\parallel}^2}{(E-E_{0,+1}+i\eta)^2}\frac{1}{D_{1,1}+\sigma_0D_{1,2}} \tag{C5}$$

and

$$\Delta I^{\perp}(E)=\mathrm{Im}\frac{2}{\pi}\frac{\mu_{\perp}^2}{(E-E_{0,-1}+i\eta)^2}\frac{1}{D_{1,1}-\sigma_0D_{1,2}}, \tag{C6}$$

with $E_{0,\pm1}=\varepsilon-2L\pm(L_a-2L_b)$.

We now assume that when the probe pulse arrives, the aggregate is in the one-exciton state $|K_0=0,\sigma_0=+1\rangle$, which may be created by pumping with parallel polarization. The denominators occurring in Eqs. (C5) and (C6) can then be written

$$D_{1,1}+D_{1,2}=-\sum_{\sigma=\pm1}\frac{1}{8(L+\sigma L_b)}S_0(p_\sigma) \tag{C7}$$

and

$$D_{1,1}-D_{1,2}=-\frac{1}{4L}S_0(p_0). \tag{C8}$$

Here the function S is given by Eq. (49) and the p_α ($\alpha=0,\pm1$) are defined in Eq. (63). Using Eqs. (50) and (C5)–(C8), we arrive at the final form of the spectra given by Eqs. (61) and (62) in the main text.

[1] A. S. Davydov, *Theory of Molecular Excitons* (Plenum, New York, 1971).
[2] V. M. Agranovich, *Theory of Excitons* (Moscow, Nauka, 1968) (in Russian).
[3] V. M. Agranovich and M. D. Galanin, in *Electronic Excitation Energy Transfer in Condensed Matter*, edited by V. M. Agranovich and A. A. Maradudin (North-Holland, Amsterdam, 1982).
[4] G. Juzeliūnas, Z. Phys. D: At., Mol. Clusters **8**, 379 (1988).
[5] J. Knoester, J. Chem. Phys. **99**, 8466 (1993).
[6] H. Ezaki, T. Tokihiro, and E. Hanamura, Phys. Rev. B **50**, 10506 (1994).
[7] F. C. Spano, Chem. Phys. Lett. **220**, 365 (1994).
[8] F. C. Spano, Chem. Phys. Lett. **234**, 29 (1995); F. C. Spano and E. Manas, J. Chem. Phys. **103**, 5939 (1995).
[9] T. Renger and V. May, Phys. Rev. Lett. **78**, 3406 (1997).
[10] G. Juzeliūnas and P. Reineker, J. Chem. Phys. **107**, 9801 (1997).
[11] G. Juzeliūnas and P. Reineker, J. Chem. Phys. **109**, 6916 (1998).
[12] J. Knoester and F. C. Spano, in *J-aggregates*, edited by T. Kobayashi (World Scientific, Singapore, 1996), p. 111.
[13] T. Meier, V. Chernyak, and S. Mukamel, J. Phys. Chem. **101**, 7332 (1997).
[14] L. D. Bakalis and J. Knoester, J. Phys. Chem. B **103**, 6620 (1999).
[15] L. Valkunas *et al.*, J. Chem. Phys. **111**, 3121 (1999).
[16] R. Gadonas, R. Danielius, R. Piskarskas, and S. Rentsch, Izv. Akad. Nauk SSSR, Ser. Fiz. **47**, 2445 (1983) [Bull. Acad. Sci. USSR, Phys. Ser. **47**, 151 (1983)].
[17] H. Fidder, J. Knoester, and D. A. Wiersma, J. Chem. Phys. **98**, 6564 (1993).
[18] A. E. Johnson, S. Kumazaki, and K. Yoshihara, Chem. Phys. Lett. **211**, 511 (1993).
[19] K. Minoshima, M. Taiji, K. Misawa, and T. Kobayashi, Chem. Phys. Lett. **218**, 67 (1994).
[20] J. R. Durrant, J. Knoester, and D. A. Wiersma, Chem. Phys. Lett. **222**, 450 (1994).
[21] R. Gagel, R. Gadonas, and A. Laubereau, Chem. Phys. Lett. **217**, 228 (1994).
[22] M. van Burgel, D. A. Wiersma, and K. Duppen, J. Chem. Phys. **102**, 20 (1995).
[23] J. Moll, S. Daehne, J. R. Durrant, and D. A. Wiersma, J. Chem. Phys. **102**, 6362 (1995).
[24] T. Pullerits, M. Chachisvilis, and V. Sundström, J. Phys. Chem. **100**, 10787 (1996).
[25] G. Scheibe, in *Optische Anregungen Organischer Systeme*, edited by W. Förster (Verlag Chemie, Weinheim, 1966), p. 109.
[26] H. Fidder, Ph.D. thesis, University of Groningen, 1993.
[27] V. Sundström, T. Gillbro, R. A. Gadonas, and A. Piskarskas, J. Chem. Phys. **89**, 2754 (1988).
[28] M. van Burgel, Ph.D. thesis, University of Groningen, 1999.
[29] I. G. Scheblykin *et al.*, Chem. Phys. Lett. **298**, 341 (1998).

[30] E. O. Potma and D. A. Wiersma, J. Chem. Phys. **108**, 4894 (1998).
[31] G. Juzeliūnas, Chem. Phys. **151**, 169 (1991).
[32] K. Misawa and T. Kobayashi, in *J-aggregates*, edited by T. Kobayashi (World Scientific, Singapore, 1996), p. 41.
[33] P. J. Reid, D. A. Higgins, and P. F. Barbara, J. Phys. Chem. **100**, 3892 (1996).
[34] A. Nabetani, A. Tomioka, H. Tamaru, and K. Miyano, J. Chem. Phys. **102**, 5109 (1995).
[35] A. Pawlik, S. Kirstein, U. De Rossi, and S. Daehne, J. Phys. Chem. B **101**, 5646 (1997).
[36] C. Spitz, Ph.D. thesis, Free University of Berlin, 1999; http://darwin.inf.fu-berlin.de/1999/15/indexe.html.
[37] J. van Kranendonk, Physica (Utrecht) **21**, 81, 749, 925 (1955).
[38] D. Dyson, Phys. Rev. **102**, 1230 (1956).
[39] V. M. Agranovich and B. S. Toshich, Zh. Eksp. Teor. Fiz. **53**, 149 (1967) [Sov. Phys. JETP **26**, 104 (1968)].
[40] J. A. Leegwater and S. Mukamel, Phys. Rev. A **46**, 452 (1992).
[41] L. D. Bakalis and J. Knoester, J. Chem. Phys. **106**, 6964 (1997).
[42] V. Ya. Chernyak, Phys. Lett. A **163**, 117 (1992).
[43] A. V. Ilinskaia and K. N. Ilinski, J. Phys. A **29**, L23 (1996).
[44] S. Mukamel, *Principles of Nonlinear Optical Spectroscopy* (Oxford, Oxford, 1995).
[45] See, e.g., N. W. Ashcroft and N. D. Mermin, *Solid State Physics* (Saunders College, Philadelphia, 1976).
[46] Equation (50) is derived in analogy to Appendix B of Ref. 11, with the exception that k now takes a different set of values.
[47] E. Daltrozzo, G. Scheibe, K. Gschwind, and F. Haimerl, Photograph. Sci. Eng. **18**, 441 (1974).
[48] P. O. J. Scherer and S. F. Fisher, Chem. Phys. **86**, 269 (1984).
[49] The apparent sign discrepancy with Ref. 11 arises because of a different choice of the sign of η.
[50] F. C. Spano, Nonlinear Opt. **12**, 275 (1995).
[51] See X. Hu and K. Schulten, Phys. Today **50**(8), 28 (1997) and references therein.
[52] No extra factor of 2 is obtained in the limiting case of two noninteracting chains, as the initial condition is still such that these two chains share only one exciton.
[53] See, e.g., T. Renger and V. May, Phys. Rev. Lett. **78**, 3406 (1997).
[54] G. Vektaris, J. Chem. Phys. **101**, 3031 (1994).